Satellite observation of dehydration in the Arctic Polar stratosphere

L. L. Pan,[1] W. J. Randel,[1] H. Nakajima,[2] S. T. Massie,[1] H. Kanzawa,[2] Y. Sasano,[2] T. Yokota,[2] T. Sugita,[2] S. Hayashida,[3] and S. Oshchepkov[2]

Received 27 September 2001; revised 10 January 2002; accepted 11 January 2002; published 18 April 2002.

[1] We report the first space-borne observation of dehydration in the Arctic polar stratosphere. In January 1997, the Improved Limb Atmospheric Spectrometer (ILAS) observed up to ~3 ppmv water vapor reduction during ice cloud formation and ~2 ppmv permanent removal of water vapor, mostly at altitudes between 23 and 26 km. In some cases, the dehydrated air was downwind from mountain wave induced Polar Stratospheric Cloud (PSC) events. Furthermore, simultaneous observations of HNO_3 and H_2O show that the gas phase reduction of HNO_3 in the Arctic (January 1997) was much smaller than that observed in the Antarctic (June 1997) when a similar level of water vapor reduction occurred. *INDEX TERMS:* 0340 Atmospheric Composition and Structure: Middle atmosphere—composition and chemistry; 0305 Atmospheric Composition and Structure: Aerosols and particles (0345, 4801); 3349 Meteorology and Atmospheric Dynamics: Polar meteorology

1. Introduction

[2] Dehydration in the winter Antarctic polar stratosphere has been observed for more than a decade by both in situ and satellite sensors [*Kelly et al.*, 1989; *Santee et al.*, 1995; *Vömel et al.*, 1995; *Nedoluha et al.*, 2000]. Due to the persistent low temperature in the Antarctic winter, dehydration is a large-scale climatological feature [*Nedoluha et al.*, 2000]. On the other hand, the occurrence of dehydration in the Arctic polar region is sporadic and has only been observed by in situ measurements in a few isolated incidents [*Vömel et al.*, 1997; *Hintsa et al.*, 1998]. In this letter, we report the first satellite observation of dehydration in the Arctic stratosphere. Also reported here are simultaneous observations of HNO_3 at the beginning of dehydration season in both hemispheres, which show a pronounced difference between HNO_3 gas phase reduction in the Arctic and the Antarctic, providing new information for investigating the PSC formation process.

[3] ILAS, onboard the Advanced Earth Observing Satellite (ADEOS), is a solar occultation instrument that has two spectrometers [*Sasano et al.*, 1999]. The spectral range of the IR spectrometer covers 6–11 μm and the visible covers 753–784 nm. ILAS retrievals provided multiple stratospheric trace gas species, including ozone (O_3), water vapor (H_2O), nitrous oxide (N_2O), and nitric acid (HNO_3), as well as aerosol extinction profiles, from November 1996 to June 1997. During this period, ILAS measurements sampled latitudes 50–70 degree N and 64–88 degree S, and provided roughly 14 profile measurements in the Arctic polar region and 14 measurements in the Antarctic polar region daily. The vertical resolution is ~1.6 km, spanning ~10–50 km altitude. The effective sampling length in the horizontal is about 230 km.

[1]National Center for Atmospheric Research, Boulder, CO, USA.
[2]National Institute for Environmental Studies, Tsukuba, Japan.
[3]Nara Women's University, Nara, Japan.

0094-8276/02/2001GL014147$05.00

[4] The results reported here are based on version 5.20 H_2O, N_2O, HNO_3, and 780 nm aerosol extinction data, all validated by correlative in situ and coincident satellite measurements [JGR ILAS special section, 2002]. IR channel aerosol extinction data are also used in PSC type analyses using a spectral fitting approach [*Oshchepkov et al.*, 2002]. Retrieval error analyses indicate that ILAS HNO_3 data are not significantly affected by the presence of aerosols. N_2O and H_2O data, on the other hand, can potentially be biased low in the presence of PSCs, due to the IR spectral overlap of gas and particles. In the absence of PSCs, the precision of the H_2O measurement for the altitude range of concern is ~10%. The estimated magnitude of PSC induced biases depends on the particle types. In particular, the PSC induced negative retrieval bias in H_2O data is not significant in the case of ice particles but can be significant in case of nitric acid trihydrate (NAT) particles. A quantitative discussion is given by *Yokota et al.* [2002]. The main results presented here are based mostly on H_2O data from the northern hemisphere (NH) in January 1997, when the majority of PSC events were identified as supercooled ternary solutions (STS) or ice [*Saitoh et al.*, 2002]. Extinction and HNO_3 data have also been carefully examined to ensure that the data points that lead to the main conclusions of this paper are not observed in the presence of NAT.

[5] Figure 1 displays a sequence of ILAS water vapor profiles for January 15–17, 1997. During each of these three days, ILAS sampled both inside and outside the Arctic polar vortex. The anomalously low water vapor events sampled inside the vortex between 23 and 26 km altitude are readily apparent in the Figure. The strong spatial correlation between H_2O minima and both temperature minima and enhanced aerosol extinction, as demonstrated in the Figure, suggests the presence of PSCs at the time of the observations. The presence of water ice PSCs is inferred. The altitudes of these events are higher than the typical altitude range of dehydration observed in the Antarctic [*Vömel et al.*, 1995; *Nedoluha et al.*, 2000]. Anomalously low water vapor was continuously observed later in the month from 17 to 26 km.

2. Observed H_2O and HNO_3 Gas Phase Reduction

[6] To search for dehydration events, we first identify all events that show anomalously low water vapor mixing ratios compared to the background values. In the absence of dehydration and PSC induced gas phase reduction, stratospheric H_2O forms a compact relationship with N_2O. In principle, the background value of H_2O can be inferred from the H_2O–N_2O relationship in the absence of PSCs and prior to significant dehydration [similar to *Kondo et al.*, 2000 in deriving the background value of HNO_3]. To eliminate data points that were measured in the presence of PSCs, we select only the measurements with co-located temperatures greater than 200 K (well above the PSC formation temperature) as the background points. Similar analyses are done for January NH and June southern hemisphere (SH) data for comparisons. Note that SH June is one month earlier than NH January in the seasonal cycle, but it is the first

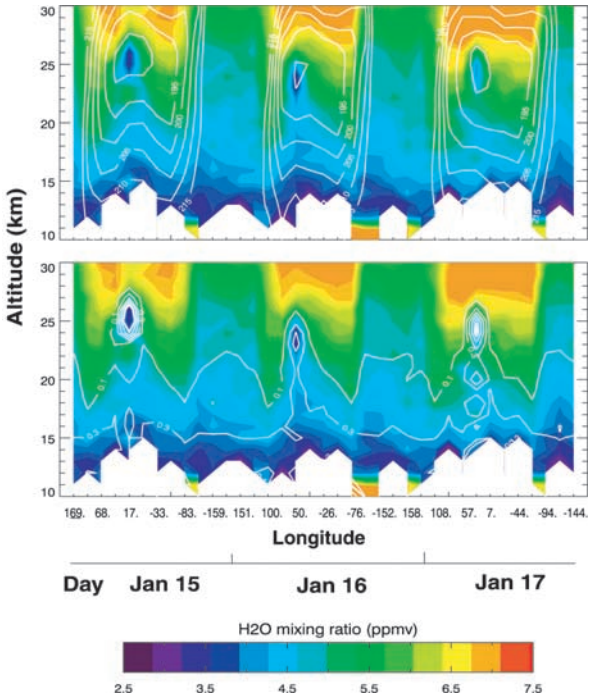

Figure 1. ILAS NH water vapor cross-section of 37 profiles along 65 degree N between January 15 and 17, 1997. Contours are co-located UKMO temperature field (top, 5 K increment) and aerosol extinction (measured by ILAS 780 nm channel) (bottom, increase 5 steps per decadal range in 10^{-3} km^{-1}).

month of the SH PSC season and the last month of the ILAS data record. In both months, the temperature criterion we used eliminates most data points that show a departure from the compact relationship. The background H_2O (HNO_3)–N_2O relationship is then determined using a polynomial fit. Figure 2 displays H_2O (HNO_3) versus N_2O for all data points between 400 K and 600 K potential temperature levels, as well as the polynomial fit to the background points, for January (NH) and June (SH). A scaled potential vorticity (sPV, in units of 10^{-4} s^{-1}), derived from the UKMO data [*Manney et al.*, 1994] is used to indicate vortex and extra-vortex air. The reason for using the entire month of PSC free data for the background fit is to avoid introducing biases due to the seasonal cycle related changes in H_2O–N_2O relationship. To shed more light on the PSC processes involved, HNO_3 anomalies are also examined. The origin of the anomalies can be further examined using their N_2O values, since N_2O has a well known stratospheric entry value in the tropics of ~315 ppbv, and a vortex value less than 150 ppbv.

[7] Deviations from the background value, ΔH_2O or ΔHNO_3, are defined as the difference between the measured value and the fit curve. We consider ΔH_2O or ΔHNO_3 larger than 2σ as cases of significant departure from the background. These cases are found in June (SH), January (NH) (Figure 2), and February (NH) 1997 (not shown). Events showing large negative ΔH_2O correspond to two different categories: 1) observations made in the presence of PSCs where the loss of water vapor may be temporary; and 2) observations made in the absence of PSCs where the loss of water vapor is permanent. We refer to both categories as gas phase reduction events but only to the latter as dehydration events.

3. Evidence of Ice Cloud Formation and Dehydration

[8] To examine quantitatively whether some of the low water vapor events during NH January were consistent with the presence of ice clouds, we investigate the relationship of observed ΔH_2O with that calculated from saturation vapor mixing ratio over ice. Figure 3a displays ΔH_2O as a function of temperature with respect to the frost point temperature (ΔT), calculated for each individual observation. Also shown in Figure 3a are corresponding saturation mixing ratios over ice for these observations calculated using a laboratory-derived formula [*Marti and Mauersburger*, 1993] (shown in Figure 3a as cyan points and curve). As expected, thermodynamics predicts that the onset of negative ΔH_2O begins only as the temperature drops to below the frost point. The data, however, show that while negative ΔH_2O events exist for a wide range of ΔT (~0–25 K), the vast majority of data are at the background level (within 2σ) until the temperature drops to below ~3–4 K above the frost point, according to the UKMO temperature data. Below this temperature, no data points were observed at the background level. Retrieval uncertainty for these data points was scrutinized and found not to have produced the observed behavior. The most likely physical explanation to the data is that a range of warm biases, with a minimum of ~3.5 K (suggested by the point where all H_2O drops to below the background value), exists in the UKMO temperature data in these cold regions. Although this warm bias is larger than typical uncertainty associated with the UKMO data, it is not uncommon for selected cold regions [e.g. *Manney et al.*, 1996]. Indeed, a wide range of warm biases, as much as 10 K, was found in analyzed temperature data (ECMWF data, which is comparable to the UKMO analyses for this month) for this particular month and location by comparison with radiosonde data and mesoscale model results [*Dörnbrack et al.*, 2001]. We further show in Figure 3a that, if a simple −3.5 K adjustment is applied to the UKMO data, the relation of negative ΔH_2O with decreasing ΔT at the low end of ΔT is consistent with the behavior of the saturation mixing ratio over ice. Furthermore, spectral analyses of ILAS aerosol extinction data, using the IR and the near visible channels, indicate that many of the events near the ice saturation curve (after the −3.5 K adjustment) in Figure 3a are consistent with the spectrum of ice particles.

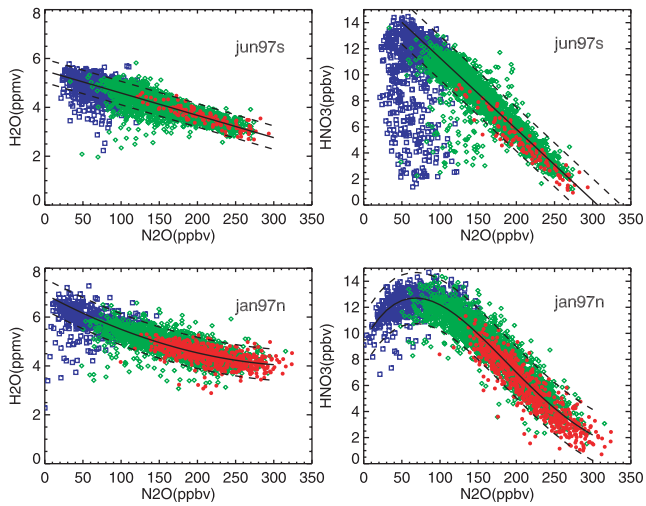

Figure 2. H_2O and HNO_3 versus N_2O for ILAS observations between 400 K and 600 K. Solid curves represent a polynomial fit to the background observations. Dashed lines represent $\pm 2\sigma$ from the fit. Colors are used to indicate vortex air (blue, sPV > 2), vortex edge (green, 1 < sPV < 2) or extra-vortex air (red, sPV < 1). The apparent shape difference between the January (NH) and June (SH) background curves of HNO_3–N_2O reflects that January is later in the vortex season and more air was sampled from higher altitudes, where N_2O has a shorter photochemical lifetime [*Michelsen et al.*, 1998].

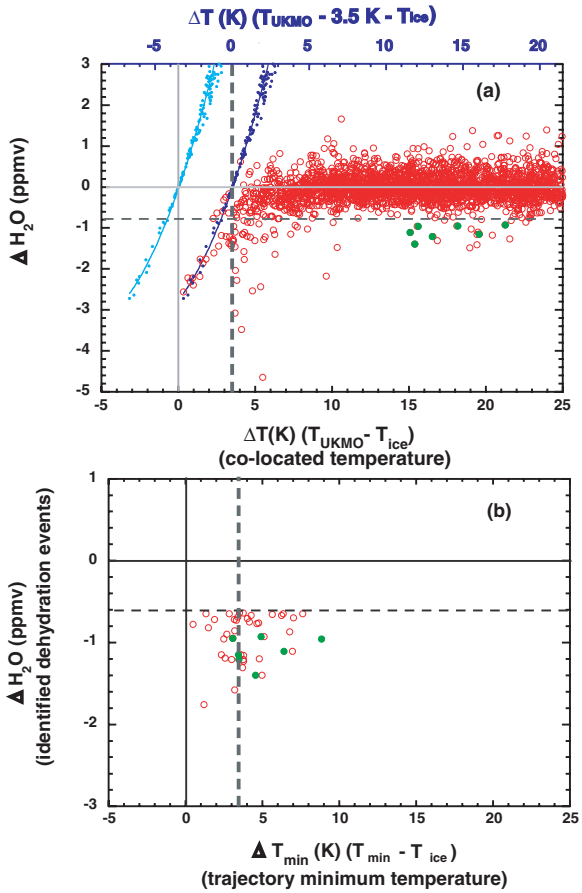

Figure 3. (a) Comparison of ILAS inferred ΔH_2O (red circles) versus ΔT (co-located temperature relative to the frost point) with the calculated saturation vapor mixing ratios using co-located UKMO T data (cyan dots and lower x-axis) and after an adjustment of −3.5 K in the T data (blue dots and upper x-axis). Cyan and blue curves are fits to the points. The dashed line (horizontal) marks -2σ from the background value; points below that are considered candidates of dehydration events. Green filled circles represent measurements of 970125. They are highlighted for their large change from high ΔT to low ΔT_{min}, as shown in (b). (b) ΔH_2O, as in (a) for those identified as dehydration events, as a function of ΔT_{min} (minimum T relative to the frost point during the past 10 days).

[9] Among the local dry anomalies observed in January (data points below the -2σ line in Figure 3a with N_2O < 150 ppbv), around 50% are identified as dehydration events using the temperature history analysis and aerosol extinction screening. Temperature histories of the past 10 days are calculated for all January events using UKMO data and a three-dimensional back trajectory model. Dry air masses that experienced near frost point temperatures and were observed in the absence of PSCs are identified as dehydrated. A total of ~40 events meet these criteria, showing up to 1.8 (±0.32) ppmv permanent loss of water (0.32 is 1σ from the background value). Their ΔH_2O values as a function of past 10 day minimum temperature relative to the frost point (ΔT_{min}) are given in Figure 3b. Detailed examinations of data show that a number of dry anomalies were observed at high ΔTs but experienced a low ΔT_{min}. A good example is given by a group of measurements on January 25, 1997, highlighted in Figure 3 (green filled circles). Most of these dehydration events were observed between altitudes 20–26 km (20–35 mbar, 500–600 K). ΔHNO_3 values for these events range from −2.3 to 1 (±0.98) ppbv, (0.98 is 1 σ from background), nearly

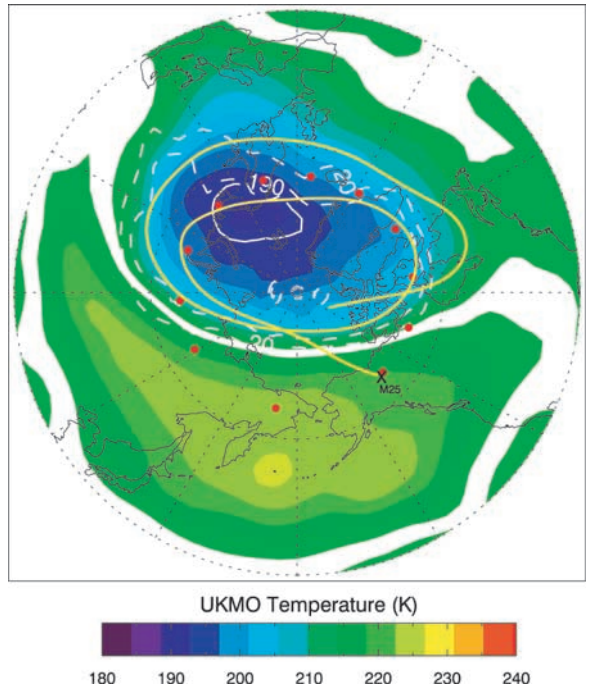

Figure 4. The yellow line indicates the10 day back trajectory of a dry event, observed on January 25 at 24 km altitude (~31 mbar) near 136 W, superposed on the UKMO temperature field on January 22 at 31 mbar. The red dots mark the ILAS measurement locations for January 22. The measurement location for the dry event observed on the 25th is marked by "**X**". The solid contour line inside the dark blue region marks the 190 K UKMO temperature. The dashed contour lines mark 20 and 25 PVU in modified PV, and are proxies for the vortex edge.

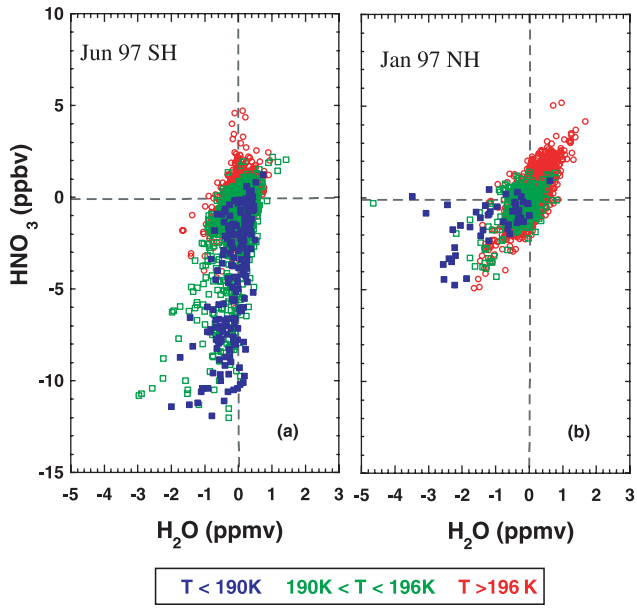

Figure 5. ΔH_2O and ΔHNO_3 for ILAS June SH (a) and January NH (b) observations between 400 K to 600 K, color-coded using the UKMO temperature (blue, T < 190 K, ice possible; green, 190 K < T < 196 K, PSC possible; red, T > 196 K, PSC free).

all distributed within $\pm 2\sigma$ of the background HNO_3 value. Note that the scatter of these events as a function of ΔT_{min} around the frost point in Figure 3b reflects the uncertainty of the temperature data and the trajectory model calculations.

[10] This group of data measured on 25th of January also serves as a good example that connects the observed dehydration with a mountain wave induced low temperature event that was not captured by the UKMO temperature data. This profile was measured over western Canada (~136 W) and anomalously dry air was found between 18 and 24 km altitudes. The trajectory analyses show that these air masses were 3 days downwind from Scandinavia. The trajectory of one of the events is illustrated in Figure 4. ΔH_2O values for these events, shown in Figure 3 (green filled circles), are from -0.93 to -1.4 (± 0.32) ppmv, when the co-located UKMO temperatures ranged from 205 K to 208 K. ILAS aerosol extinction values for these events are at background levels, indicating the absence of PSCs. Back trajectory calculations using UKMO analyses indicate that these air masses experienced their temperature minimum (~190 K in UKMO analyses) over Northern Scandinavia three days earlier (January 22). During this time period, a ground based Lidar near Kiruna, Sweden (68°N, 21°E) observed intense mountain-wave induced PSCs. Mesoscale temperature simulations, supported by nearby radiosonde data, showed that the mountain-wave induced temperature anomaly reached as low as 178 K (7 K below local frost point temperature) at the 30 mbar level [*Dörnbrack et al.*, 2001]. The fact that dry air masses were measured three days later at temperatures much higher than the frost point indicates that the ice particles grew large enough to sediment before total evaporation. These events probably resulted from the combination of mountain-wave induced low temperature anomaly and the synoptic scale low temperature pool inside the polar vortex.

4. Discussion of HNO_3 Gas Phase Reduction in the Arctic

[11] In addition to the water vapor anomalies, Figure 2 shows a strong contrast of HNO_3 anomalies between the Arctic and the Antarctic. Although it is well known that the perturbation of gas phase HNO_3 is in general much smaller in the Arctic [e.g. *Santee et al.*, 1995], it is somewhat surprising that only 3–5 ppbv of HNO_3 gas phase reduction was observed during the occurrence of ice cloud formation and dehydration. The different characteristics of ΔHNO_3 versus ΔH_2O between the Antarctic (June) and the Arctic (January) are further highlighted in Figure 5. Note that these ΔH_2O and ΔHNO_3 values are not equivalent to dehydration and denitrification, but represent gas phase reduction, many of which may be due to the presence of PSCs. The likelihood of PSCs is indicated by the colors in Figure 5, based on their co-located temperatures. It is apparent that while the inferred ΔH_2O are comparable for these two months, the ΔHNO_3 in the NH (January) are much smaller (~35% of the HNO_3 background value in the NH compared to over 90% in the SH).

[12] In light of recent studies showing that the growth of solid nitric acid containing particles requires 6–7 days [*Fahey et al.*, 2001], and that the growth rate peaks in a narrow temperature window (190–192 K at 500 K altitude) [*Tabazadeh et al.*, 2001], we examined the parcels' temperature histories. The results show that, typically, the Antarctic air masses experienced a stable low temperature (below critical temperature for NAT) for several days, whereas the Arctic trajectories show a more rapid cooling and warming (reflecting the fact that the Arctic cold pool is smaller and asymmetric in shape). On one hand, the much smaller ΔHNO_3 produced under these conditions are consistent with the fact that these Arctic parcels did not stay long enough in the temperature window that is optimal for solid nitric acid containing particles to form. On the other hand, it brings out a new aspect that the freezing of water is a faster process than the formation of nitric acid containing particles. In principle, this can lead to the situation where dehydration may occur before denitrification, or in some cases, without denitrification. These results also show that without persistent low temperatures, the presence of ice particles does not necessarily produce efficient denitrification. Furthermore, the fact that only around 3–5 ppbv of HNO_3 gas phase reduction (likely due to STS, [*Saitoh et al.*, 2002]) was observed under conditions of ice cloud formation challenges the current understanding of STS formation. To understand the future changes in Arctic stratospheric ozone, these new aspects need to be investigated by theoretical modeling and laboratory experiments.

[13] **Acknowledgments.** We thank A. Dörnbrack, D. Hanson, B. Ridley and A. Tabazadeh for helpful discussions. This work is supported in part by the National Science Foundation through its support to the University Corporation for Atmospheric Research, by the NASA Upper Atmosphere Research Satellite guest investigator program, and by the NASA Atmospheric Chemistry Modeling and Analysis Program.

References

Dörnbrack, A., et al., Relevance of mountain wave cooling for the formation of polar stratospheric clouds over Scandinavia: Mesoscale dynamics and observations for January 1997, *J. Geophys. Res.*, *106*, 1569, 2001.

Fahey, D. W., et al., The detection of large HNO_3-containing particles in the winter Arctic stratosphere, *Science*, *291*, 1026–1031, 2001.

Hintsa, E. J., et al., Dehydration and denitrification in the Arctic polar vortex during the 1995–1996 winter, *Geophys. Res. Lett.*, *25*, 501, 1998.

Kelly, K. K., et al., Dehydration in the lower Antarctic stratosphere during late winter and early spring 1987, *J. Geophys. Res.*, *94*, 11,317, 1989.

Kondo, Y., H. Irie, M. Koike, and G. E. Bodeker, Denitrification and nitrification in the Arctic stratosphere during the winter of 1996–1997, *Geophys. Res. Lett.*, *27*, 337–340, 2000.

Manney, G. L., R. W. Zurek, A. O'Neil, and R. Swinbank, On the motion of air through the stratospheric polar vortex, *J. Atmos. Sci.*, *51*, 2973–2994, 1994.

Manney, G. L., et al., Comparison of U. K. Meteorological Office and U.S. National Meteorological Center stratospheric analyses during northern and southern winter, *J. Geophys. Res.*, *101*, 10,311–10,334, 1996.

Marti, J., and K. Mauersburger, A survey and new measurements of ice vapor pressure at temperature between 170 and 250 K, *Geophys. Res. Lett.*, *20*, 363–366, 1993.

Michelsen, H. A., G. L. Manney, M. R. Gunson, and R. Zander, Correlations of stratospheric abundances of NO_y, O_3, N_2O, and CH_4 derived from ATMOS measurements, *J. Geophys. Res.*, *103*, 28,347–28,359, 1998.

Nedoluha, G. E., et al., POAM III measurements of dehydration in the Antarctic lower stratosphere, *Geophys. Res. Lett.*, *27*, 1683–1686, 2000.

Oshchepkov, S., Y. Sasano, T. Yokota, and H. Nakajima, Retrieval of stratospheric aerosol composition from spectral limb scanning observations at the infrared gas window channels. Part 1. Inversion method and numerical tests, submitted to *J. Geophys. Res.*, 2002.

Saitoh, N., et al., Characteristics of Arctic polar stratospheric clouds in the winter of 1996/1997 inferred from ILAS measurements, *J. Geophys. Res.*, in press, 2002.

Santee, M. L., et al., Interhemispheric differences in polar stratospheric HNO_3, H_2O, ClO, and O_3, *Science*, *267*, 849–852, 1995.

Sasano, Y., et al., Improved Limb Atmospheric Spectrometer (ILAS) for stratospheric ozone layer measurements by solar occultation technique, *Geophys. Res. Lett.*, *26*, 197–200, 1999.

Tabazadeh, A., et al., Role of the stratospheric polar freezing belt in denitrification, *Science*, *291*, 2591–2594, 2001.

Vömel, H., et al., Evolution of the dehydration in the Antarctic stratospheric vortex, *J. Geophys. Res*, *100*, 13,919–13,926, 1995.

Vömel, H., et al., Dehydration and sedimentation of ice particles in the Arctic stratospheric vortex, *Geophys. Res. Lett.*, *24*, 795–798, 1997.

Yokota, T., et al., Improved Limb Atmospheric Spectrometer (ILAS) data retrieval algorithm for Version 5.20 gas profile products, *J. Geophys. Res.*, in press, 2002.

L. L. Pan, W. J. Randel, and S. T. Massie, National Center for Atmospheric Research, Boulder, CO 80307, USA.

H. Nakajima, H. Kanzawa, Y. Sasano, T. Yokota, T. Sugita, and S. Oshchepkov, National Institute for Environmental Studies, Tsukuba, Japan.

S. Hayashida, Nara Women's University, Nara, Japan.